Monthly Notices
of the
ROYAL ASTRONOMICAL SOCIETY

MNRAS **448,** 1893–1899 (2015) doi:10.1093/mnras/stv143

The powerful jet of an off-nuclear intermediate-mass black hole in the spiral galaxy NGC 2276

M. Mezcua,[1,2,3]★ T. P. Roberts,[4] A. P. Lobanov[5]† and A. D. Sutton[4]

[1]*Harvard-Smithsonian Center for Astrophysics (CfA), 60 Garden Street, Cambridge, MA 02138, USA*
[2]*Instituto de Astrofísica de Canarias (IAC), E-38200 La Laguna, Tenerife, Spain*
[3]*Department Astrofísica, Universidad de La Laguna, E-38206 La Laguna, Tenerife, Spain*
[4]*Department of Physics, University of Durham, South Road, Durham DH1 3LE, UK*
[5]*Max Planck Institute for Radio Astronomy, Auf dem Hügel 69, D-53121 Bonn, Germany*

Accepted 2015 January 20. Received 2015 January 15; in original form 2014 October 21

ABSTRACT

Jet ejection by accreting black holes is a mass invariant mechanism unifying stellar and supermassive black holes (SMBHs) that should also apply for intermediate-mass black holes (IMBHs), which are thought to be the seeds from which SMBHs form. We present the detection of an off-nuclear IMBH of $\sim 5 \times 10^4$ $M_\odot$ located in an unusual spiral arm of the galaxy NGC 2276 based on quasi-simultaneous *Chandra* X-ray observations and European VLBI Network (EVN) radio observations. The IMBH, NGC2276-3c, possesses a 1.8 pc radio jet that is oriented in the same direction as large-scale (∼650 pc) radio lobes and whose emission is consistent with flat to optically thin synchrotron emission between 1.6 and 5 GHz. Its jet kinetic power (4×10^{40} erg s^{-1}) is comparable to its radiative output and its jet efficiency (≥46 per cent) is as large as that of SMBHs. A region of ∼300 pc along the jet devoid of young stars could provide observational evidence of jet feedback from an IMBH. The discovery confirms that the accretion physics is mass invariant and that seed IMBHs in the early Universe possibly had powerful jets that were an important source of feedback.

Key words: accretion, accretion discs – black hole physics – ISM: jets and outflows – X-rays: binaries – radio continuum: general.

1 INTRODUCTION

Intermediate-mass black holes (IMBHs) constitute the missing link between stellar-mass and supermassive black holes (SMBHs) and are the potential long-sought seeds from which SMBHs grow. IMBHs could form either from the death of very massive and short-lived stars, the direct collapse of a pre-galactic gas disc, or the collapse of dense stellar clusters, and then grow either through hierarchical merging or secular gas accretion (Volonteri 2010). They should thus be present in the nuclei of low-mass galaxies, as predicted from BH mass ($M_{\rm BH}$)-scaling relations (e.g. Graham & Scott 2013); in dense star-forming regions in spiral galaxies; and in the haloes of large galaxies (e.g. after tidal stripping of merging low-mass satellite galaxies). SMBHs with masses up to 10^9 $M_\odot$ already existed when the Universe was less than ∼1 Gyr old (e.g. Mortlock et al. 2011). To reach this mass in such a short time, seed IMBHs must have undergone short phases of growth above the Eddington rate coupled with enhanced star formation triggered by jets or outflows (Volonteri & Silk 2014) or supra-exponential accretion (Alexander & Natarajan 2014). Cosmological simulations show that the radiative and mechanical feedback from an accreting IMBH regulate its growth and deprive the inner core of the galaxy of cold star-forming gas (Kim et al. 2011; Dubois et al. 2012). However, the detection of IMBHs and, in particular, of jet emission from IMBHs is scarce and no evidence of its feedback effects has hitherto been observed.

The best observational evidence for IMBHs has been found in the nuclei of low-mass spiral and dwarf galaxies (Dong et al. 2007; Greene & Ho 2007; Thornton et al. 2008; Reines, Greene & Geha 2013; Schramm et al. 2013; Yuan et al. 2014) and in ultraluminous X-ray sources (ULXs; Farrell et al. 2009). Evidence is mounting that the high X-ray luminosity of the majority of ULXs can be explained by stellar-mass BHs accreting at around or above the Eddington limit (e.g. Gladstone, Roberts & Done 2009; Sutton, Roberts & Middleton 2013; Motch et al. 2014). However, those ULXs with $L_{\rm X} > 5 \times 10^{40}$ erg s^{-1} remain difficult to explain as super-Eddington accretion on to stellar-mass BHs, and display X-ray emission properties consistent with IMBHs either accreting in a sub-Eddington hard state (Sutton et al. 2012) or in an intermediate

★ E-mail: mar.mezcua@cfa.harvard.edu
† Visiting Scientist, University of Hamburg/Deutsches Elektronen Synchrotron Forschungszentrum.

state (Pasham, Strohmayer & Mushotzky 2014). One such object is a ULX in NGC 2276 (NGC2276-3c for simplicity), which had a peak X-ray luminosity of up to $\sim 6 \times 10^{40}$ erg s^{-1} when observed with the *XMM-Newton* satellite (see Section 2.2 for further details). If they are in the sub-Eddington hard or intermediate states, accreting BHs are expected to emit radio jets. Observational evidence for compact or transient jet radio emission has been found in a few ULXs (Mezcua & Lobanov 2011; Cseh et al. 2012, 2014; Webb et al. 2012; Mezcua et al. 2013a, 2014; Middleton et al. 2013). The best evidence for the presence of a radio jet in an off-nuclear IMBH comes from ESO 243-49 HLX-1, which shows flaring radio emission when appearing to transition from the low/hard X-ray state to the high/soft X-ray state (Webb et al. 2012; Cseh et al. 2015). However, observational evidence of extended, steady jet radio emission from IMBHs has so far only been found in the nuclear IMBHs NGC 4395 (jet extent ∼0.3 pc; Wrobel & Ho 2006) and GH10 (jet extent <320 pc; Wrobel et al. 2008). For the ULX NGC2276-3c, extended radio emission formed by two lobes of total size ∼650 pc was detected with the Karl G. Jansky Very Large Array (VLA). The X-ray source is located in between the two radio lobes, suggesting the presence of a central BH powering a two-sided radio jet (Mezcua et al. 2013c). Using the X-ray peak luminosity, an $M_{\rm BH} \geq 4700$ M$_\odot$ was estimated assuming 10 per cent Eddington accretion (Sutton et al. 2012). The VLA observations could thus have revealed the largest radio jet ever detected from an IMBH.

In this paper, we report quasi-simultaneous very long baseline interferometry (VLBI) radio observations with the European VLBI Network (EVN) and X-ray observations with the *Chandra* X-ray observatory of NGC2276-3c, which reveal the detection of a parsec-scale radio jet with an orientation consistent with that of the VLA radio lobes and allow us to estimate an $M_{\rm BH}$ in the IMBH range. A description of the observations and results is provided in Section 2. The discussion of the results and final conclusions are given in Sections 3 and 4, respectively.

2 OBSERVATIONS, ANALYSIS AND RESULTS

2.1 EVN observations

EVN observations of NGC2276-3c were carried out during two 6-h observing runs on 2013 May 23 and June 3 at 5 and 1.6 GHz, respectively (experiments EM106A and EM106B). The observations were carried out in the phase-reference mode, alternating scans between the target source and a nearby ($\Delta\theta \sim 3.^\circ2$) compact source used as phase calibrator (J0508+8432). In total, ∼3 h were spent on NGC2276-3c at both frequencies. The bright radio source 4C+39.25 was also observed to be used as fringe finder and bandpass calibrator. The data were recorded at a rate of 1024 Mbps in dual circular polarization, using eight sub-bands (each 16 MHz in width and split into 32 spectral channels), and correlated at the EVN Correlator Facility of the Joint Institute for VLBI in Europe (JIVE) with an averaging time of 1 s. Amplitude calibration (using system temperatures and antennas gains) and fringe fitting were performed using the AIPS software. Ionospheric calibration was also applied at both frequencies. Radio maps at 1.6 GHz (Fig. 1d) and 5 GHz were obtained using hybrid imaging with CLEAN deconvolution and the natural weighting of the data. At 1.6 GHz, radio emission at a 9σ level is detected in between the two peaks of the radio lobes previously detected with the VLA (Fig. 1b). The emission has a flux density of 65 ± 16 μJy, from which we derive an integrated radio luminosity $L_{1.6\rm GHz} = 1.4 \times 10^{35}$ erg s^{-1} assuming a distance to NGC 2276 of 33.3 Mpc (Sutton et al. 2012). This spectral luminosity is of the same order as that of the IMBH in NGC 4395 (Wrobel & Ho 2006) and one order of magnitude lower than the radio luminosity of parsec-scale jets in active galactic nuclei (AGN) residing in spiral galaxies (e.g. NGC 1097; Mezcua & Prieto 2014). The emission was fitted by a two-dimensional elliptical Gaussian component, which is centred at RA(J2000) = $07^{\rm h}26^{\rm m}48\overset{\rm s}{.}092 \pm 0\overset{\rm s}{.}001$, Dec.(J2000) = $+85^\circ45'48\overset{''}{.}9180 \pm 0\overset{''}{.}0006$, has a major axis deconvolved size of 11.3 mas (∼1.8 pc) oriented at a position angle of 78° and a brightness temperature $T_{\rm B} = 1.5 \times 10^5$ K. The deconvolved size of 11.3 mas is larger than the resolution limit[1] of 5.4 mas, implying that the emission is resolved along the major axis. Its orientation, at a position angle of 78° north-through-east, is consistent with that of the VLA radio lobes. The finding of $T_{\rm B} > 10^5$ rules out thermal free–free emission (of typically 10^4 K) from e.g. H II regions, suggesting that the emission may be non-thermal. The same result is obtained when performing hybrid imaging with CLEAN deconvolution plus self-calibration loops, which proves that the extended emission is not caused by phase errors.

The radio map at 5 GHz was produced using the data from baselines shorter than 20 Mλ (1200 km) in order to improve the detection of extended emission. A restoring beam of 16.4 × 13.1 mas full width at half-maximum (FWHM) was used in order to match that of the 1.6-GHz radio map and derive the spectral index. A compact component of flux density 39 ± 18 μJy and radio luminosity of $L_{5\,\rm GHz} = 2.6 \times 10^{35}$ erg s^{-1} is detected at the ∼8σ level. The component is centred at RA(J2000) = $07^{\rm h}26^{\rm m}48\overset{\rm s}{.}093 \pm 0\overset{\rm s}{.}001$, Dec.(J2000) = $+85^\circ45'48\overset{''}{.}912 \pm 0\overset{''}{.}001$. It has a size of 13.3 × 12.7 mas oriented at a position angle of 11° and $T_{\rm B} = 1.1 \times 10^4$ K. The total positional errors of the target source are estimated at both frequencies as a quadratic sum of the positional error of the target source in the phase-referenced map, the positional error of the phase-reference calibrator and the error of phase referencing due to ionospheric effects. This yields a total positional error for NGC2276-3c of 3.5 mas at 1.6 GHz and 2.4 mas at 5 GHz. The position of the components identified at each frequency coincides within these positional errors. A spectral index $\alpha = -0.5 \pm 0.2$, $S_\nu \propto \nu^\alpha$, is derived from the integrated flux densities at 1.6 and 5 GHz. Using the peak densities, an even flatter spectral index $\alpha = -0.3 \pm 0.1$ would be obtained. In both cases, the spectral index is consistent with flat to optically thin synchrotron emission.

2.2 *Chandra* observations

A *Chandra* X-ray observation (ID 15648) was carried out quasi-simultaneously with (i.e. started within one day of the completion of) the 5-GHz radio observations, with the target placed at the nominal aim-point on the S3 chip of the ACIS-S array. The source was observed for an exposure time of 25 ks, and the observation was processed using standard tools in CIAO v4.6, with calibration files from CALDB v4.6.1.1. In total, 188 counts were detected from the ULX, yielding a 0.3–10 keV count rate of $(7.5 \pm 0.6) \times 10^{-3}$ count s^{-1}. The source was also previously detected by *Chandra* on 2004 June 23 (ID 4968), when it had a count rate of $\sim 2.6 \times 10^{-3}$ count s^{-1} (Wolter et al. 2011; Sutton et al. 2012). Hence, NGC2276-3c was ∼3 times brighter in the new observation than in the only previous observation in which it was resolved from its neighbouring ULXs.

[1] The resolution limit is given by $\theta_{\rm lim} = \frac{2}{\pi}[\pi b_{\rm maj} b_{\rm min} \ln((\rm SNR + 1)/\rm SNR)]^{1/2}$, where $b_{\rm maj}$ and $b_{\rm min}$ are the beam major and minor axis, respectively, and SNR, the signal-to-noise ratio (Lobanov 2005).

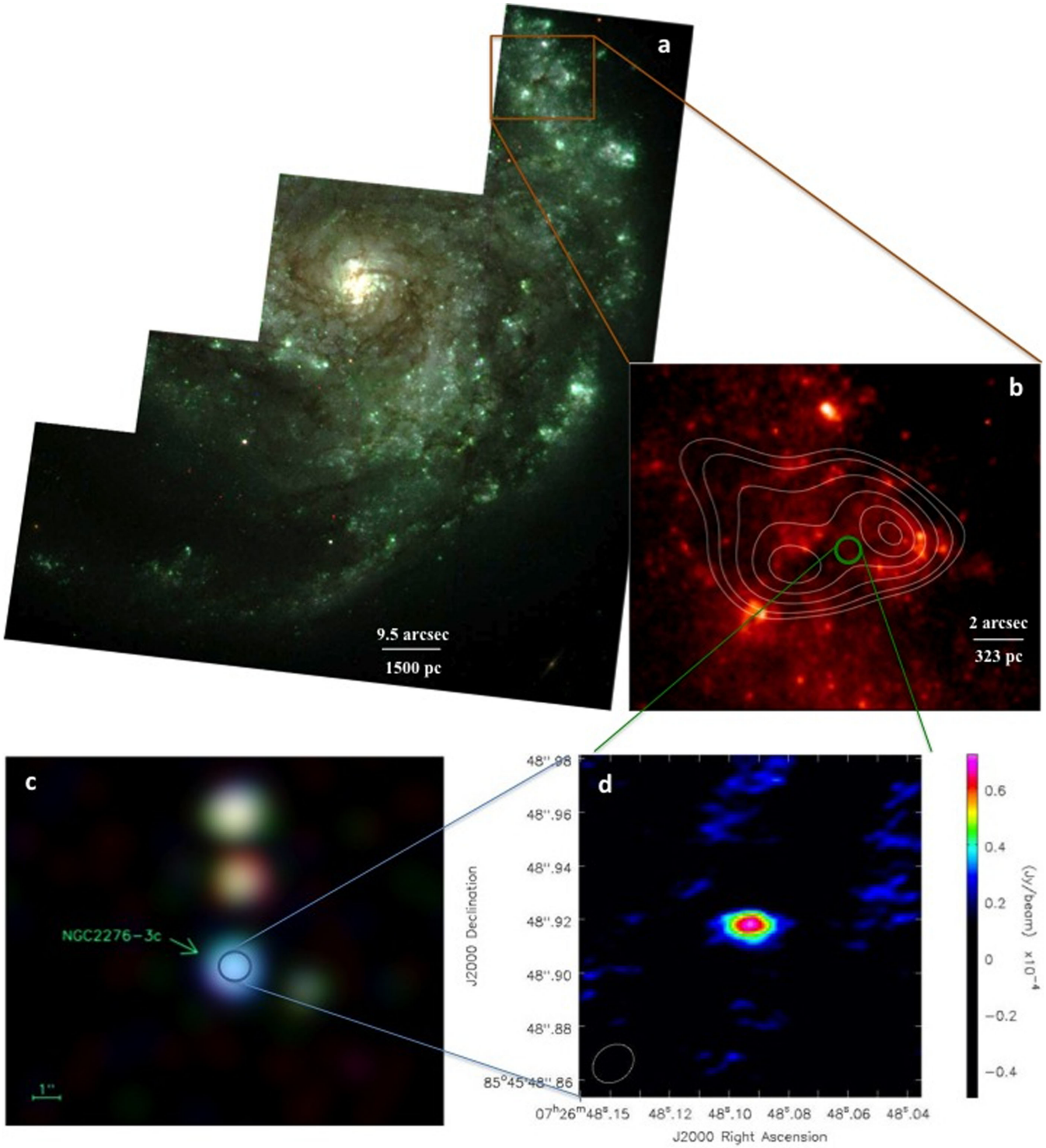

Figure 1. (a) Three-colour image of the western arm of NGC 2276 where the ULX is located. The image has been created using three filters of the Wide Field Planetary Camera 2 on the *HST*: *F*814*W* in red (∼0.8 μm), *F*606*W* in green (∼0.6 μm) and *F*550*W* in blue (∼0.55 μm). (b) *I*-band (∼0.8 μm) *HST* image of the region where the ULX NGC2276-3c is located. The 5-GHz VLA radio lobes (Mezcua et al. 2013c) are overplotted as (5,6,7,8,9,10) times the off-source rms noise of 0.04 mJy beam^{-1}. The *Chandra* X-ray position is marked with a green circle of ∼1 arcsec diameter. The VLA beam size is 4.6 arcsec × 3.5 arcsec. (c) *Chandra* red (0.2–1.5 keV), green (1.5–2.5 keV) and blue (2.5–8 keV) image convolved with an ∼2 arcsec FWHM Gaussian. The position of NGC2276-3c is marked with a blue circle of ∼1 arcsec diameter. (d) EVN 1.6 GHz image of NGC2276-3c. The synthesized beam size is 16.4 × 13.1 mas oriented at a P.A. of −52°. The off-source rms noise is 8 μJy beam^{-1}.

We used XSPEC v12.8.1 to fit models to the binned X-ray spectrum. Both an absorbed power-law and a multicolour-disc (MCD) model were used to fit the data. In both cases, we included two absorption components: the first was set equal to the line-of-sight Galactic column density in the direction of NGC 2276 (5.52×10^{20} cm^{-2}; Dickey & Lockman 1990), whilst the other was free to vary, to model any intrinsic absorption in the source and/or the host galaxy. The fit statistics for the power-law and MCD were χ^2/degrees of freedom = 13.7/15 and 13.2/15, respectively. We extracted the best-fitting model parameters from the absorbed power-law and MCD. These were $N_{\rm H} = 1.3^{+0.5}_{-0.4} \times 10^{22}$ cm^{-2} and $\Gamma = 1.4 \pm 0.3$ for the power law, and $N_{\rm H} = (0.9 \pm 0.3) \times 10^{22}$ cm^{-2} and $k_{\rm B}T_{\rm in} = 2.4^{+1.0}_{-0.5}$ keV for the MCD. All of these parameters are consistent with the values reported by Sutton et al. (2012) for the previous *Chandra* observation, and only the normalizations differ significantly. The parameters are also consistent, within the errors, with those obtained when fitting the unbinned data using the C-statistic in XSPEC for Poisson data with a Poisson background.[2] Interestingly, the high disc temperature from the MCD fit is similar to that seen in Galactic black holes in the steep power-law state (bright intermediate states), and so appears somewhat too high for an IMBH. However, we note that the moderate data quality may simply be insufficient to reject an MCD fit to a power-law spectrum in this case.

We estimated observed X-ray fluxes from the absorbed power-law model, which we converted to luminosities. These are $L_{0.3-10\,{\rm keV}} = 1.8^{+0.3}_{-0.2} \times 10^{40}$ erg s^{-1} and $L_{2-10\,{\rm keV}} = 1.6^{+0.3}_{-0.2} \times 10^{40}$ erg s^{-1}. This corresponds to an increase in luminosity of $\sim$3.5 from the 2004 *Chandra* observation. Although NGC2276-3c has increased in X-ray luminosity, the total luminosity of this and the other nearby point sources (see below) is still less than that of the extreme luminosity ULX observed by *XMM–Newton* (2XMM J072647.9+854550; 0.3–10 keV luminosity of $(6.1 \pm 0.3) \times 10^{40}$ erg s^{-1}), meaning that at least one of the point sources detected by *Chandra* within the *XMM–Newton* beam must have previously been even more luminous in X-rays. Given the location of the centroid of the *XMM–Newton* detection (cf. fig. 1 of Sutton et al. 2012), it is likely that the brighter source was either 3b or 3c.

We also examined the *Chandra* light curve of the ULX to test for evidence of variability. However, the 3σ upper limit on the rms fractional variability is very unconstrained at $\sim$0.6. Although the data are relatively poor, we note that the characteristics of a hard accretion state – a power-law spectral form with $\Gamma \sim 1.7$ and rms variability at the 10–20 per cent level – are well within the range of allowed parameters we have derived. Given the detection of a radio jet characteristic of the hard state, a thermal-dominant state appears unlikely, although we cannot statistically rule out an accretion disc-like spectrum (but we again note that the derived temperature is somewhat higher than typical for a thermal-dominant state). We can therefore conclude that the data are consistent with a hard accretion state.

Motivated by the large change in the X-ray luminosity of NGC2276-3c, we also tested whether the neighbouring sources (3a and 3b in Sutton et al. 2012) had varied too. To do this, we extracted energy spectra from the latest *Chandra* observation using the same method as above. We then fitted both of the ungrouped spectra with a doubly absorbed power law, by minimizing the modified Cash-statistic (which allows for a background spectrum) in XSPEC. We find that source 3a is well modelled by a power-law spectrum with $N_{\rm H} = (5 \pm 2) \times 10^{21}$ cm^{-2}, $\Gamma \sim 1.7 \pm 0.2$ and observed 0.3–10 keV luminosity $L_{\rm X} = (1.3 \pm 0.2) \times 10^{40}$ erg s^{-1}, whereas source 3b has $N_{\rm H} = (6 \pm 2) \times 10^{21}$ cm^{-2}, $\Gamma = 2.2 \pm 0.4$ and observed 0.3–10 keV luminosity $L_{\rm X} = 5.5^{+1.1}_{-0.9} \times 10^{39}$ erg s^{-1}. These model parameters and fluxes are consistent (within the 90 per cent uncertainty regions) with the previous values from the 2004 observation.

3 DISCUSSION

3.1 The nature of NGC2276-3c

The spatial coincidence of the EVN non-thermal radio emission with the location of unresolved, hard X-ray emission constitutes one of the most compelling radiative signatures of an accreting BH. It also permits a measurement of the $M_{\rm BH}$ using the Fundamental Plane of BH accretion, which is a correlation between core radio luminosity, X-ray luminosity and $M_{\rm BH}$ valid from stellar to SMBHs in the hard X-ray spectral state, where steady jet emission is ubiquitous. For this purpose, we use the empirical Fundamental Plane dependence of Gültekin et al. (2009, equation 3), which is the only one that has been tested in the IMBH range (Gültekin et al. 2014). Using the EVN radio luminosity at 5 GHz and the *Chandra* X-ray luminosity in the 2–10 keV band, we obtain $M_{\rm BH} = 5 \times 10^4$ M$_\odot$ with a scatter of 0.7 dex, which confirms that the ULX harbours an IMBH (Fig. 2). The mass obtained using other Fundamental Plane correlations (e.g. Merloni, Heinz & di Matteo 2003; Miller-Jones et al. 2012; Plotkin et al. 2012) is also consistent with an IMBH, though we note that these have not been proven to be valid in the IMBH range and sometimes assume certain accretion physics that do not necessarily apply to NGC2276-3c. Further uncertainties also arise from the discovery of a second track in the Fundamental Plane (Gallo, Miller & Fender 2012) and of no dependence of the radio/X-ray correlation with BH mass in X-ray binaries (XRBs; Gallo et al. 2014).

To further probe the nature of the source, we also calculate the $R_{\rm X}$ ratio of 5-GHz radio emission to 2–10 keV X-ray

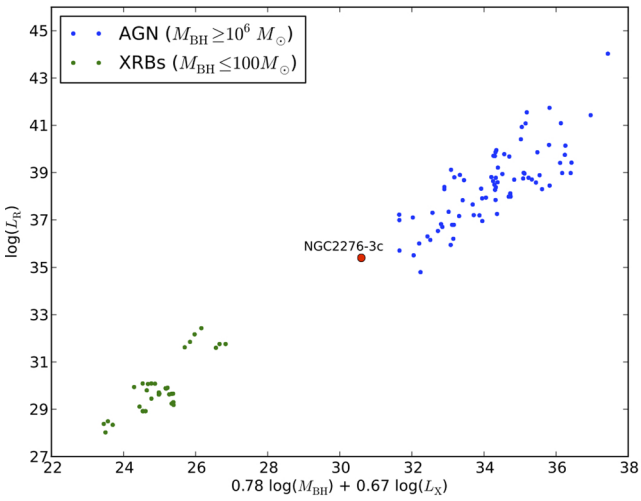

Figure 2. Fundamental Plane of BH accretion from Gültekin et al. (2009) extending from XRBs hosting stellar-mass BHs (green dots) to AGN hosting SMBHs (blue dots). The sample of XRBs and AGN is taken from Merloni et al. (2003). A clear gap in the correlation is observed in the IMBH range, where NGC2276-3c is located.

[2] https://heasarc.gsfc.nasa.gov/xanadu/xspec/manual/XSappendixStatistics.html

emission: $R_X = \nu L_\nu(5\ \mathrm{GHz})/L_X(2\text{–}10\ \mathrm{keV})$ (Terashima & Wilson 2003). XRBs have typical values of $\log R_X < -5.3$, low-luminosity AGN have $-3.8 < \log R_X < -2.8$ and supernova remnants have $\log R_X \sim -2$ (e.g. Mezcua, Lobanov & Martí-Vidal 2013b; see also table 3 in Mezcua et al. 2013a and references therein). NGC2276-3c has $\log R_X = -4.9$, which falls in the range -5.3 to -3.8 expected for IMBHs (Mezcua et al. 2013a) and rules out a SMBH nature. A background AGN is also disfavoured by the location of the ULX within a spiral arm in which the VLA radio lobes and the X-ray source appear to line up with a cavity in the optical emission (Fig. 1b), and by the low probability of a chance alignment with a background source calculated from the VLA field (Mezcua et al. 2013c). It should be noted that the fact that this ULX has a large-scale (lobe-like) structure and a small-scale jet indicates that other ULX masses derived for similar sources using VLA flux density measurements may be biased towards higher values (since the radio luminosity obtained from VLA measurements can be overestimated).

3.2 Eddington ratio and accretion rate

The Fundamental Plane has been applied under the assumption that the source is accreting at a sub-Eddington rate. The Eddington ratio is given by $k_{\rm bol}L_X/[1.38 \times 10^{38} \times (M_{\rm BH}/\mathrm{M}_\odot)]$ where $k_{\rm bol}$ is the 2–10 keV bolometric correction factor and ranges from 5 (Marchese et al. 2012) to ∼30 for AGN with Eddington ratios ≤0.1 (Vasudevan & Fabian 2009) and $k_{\rm bol} \sim 1$ for XRBs (e.g. Migliari & Fender 2005). Assuming $k_{\rm bol} = 5$ for NGC2276-3c (i.e. in between those of AGN and XRBs), and using $M_{\rm BH} = 5 \times 10^4$ $\mathrm{M}_\odot$ and the 2–10 keV X-ray luminosity, yields an Eddington ratio $\sim 10^{-2}$. The possibility that NGC2276-3c is accreting at a higher Eddington rate should also be considered. If the source is accreting at the Eddington limit, it has $M_{\rm BH} \geq 725\ \mathrm{M}_\odot$, which still puts NGC2276-3c in the IMBH range. Even in the most conservative scenario that all the luminosity is emitted in the 2–10 keV X-ray band ($k_{\rm bol} = 1$) and there is no intrinsic absorption, the source would have $M_{\rm BH} \geq 145\ \mathrm{M}_\odot$. Therefore, NGC2276-3c would qualify as an IMBH even if it were accreting at its Eddington rate. However, we now know that ULXs can be powered by super-Eddington emission from a stellar-mass BH (e.g. Liu et al. 2013; Middleton et al. 2013). Given that the maximal emission from a super-Eddington accretion disc is a factor ∼20 above the Eddington luminosity (e.g. Mineshige & Ohsuga 2011[3]), in the case of NGC2276-3c we would require a massive stellar BH (>31 $\mathrm{M}_\odot$) to power the peak X-ray luminosity. We note, though, that the presence of such a powerful, extended radio jet is unprecedented for a ULX accreting at super-Eddington rates. Empirical evidence that BHs with supercritical accretion can have powerful jets has so far only been found in two stellar-mass BHs (S26, in the nearby galaxy NGC 7793, Pakull, Soria & Motch 2010; and MQ1, in the spiral galaxy M83, Soria et al. 2014).

An estimate of the absolute accretion rate (i.e. in terms of mass accreted) can be obtained as $\dot{M}_{\rm BH} = k_{\rm bol}L_X/(\eta c^2)$ assuming a typical efficiency (η) of conversion of rest mass into energy of 10 per cent. Taking $k_{\rm bol} = 5$ yields $\dot{M}_{\rm BH} = 1.5 \times 10^{-5}\ \mathrm{M}_\odot\ \mathrm{yr}^{-1}$, which is close to the Eddington accretion rate of a 1000 $\mathrm{M}_\odot$ BH ($2 \times 10^{-5}\ \mathrm{M}_\odot\ \mathrm{yr}^{-1}$). The accretion rate is also one to two orders of magnitude higher than that of sub-Eddington to nearly Eddington accreting stellar-mass BHs with radio jet emission (e.g. IC10 X-1, Cseh et al. 2012; GRS1915+105, Rushton et al. 2010), which favours an IMBH nature for NGC2276-3c. However, we note that it is also one order of magnitude smaller than that of the super-Eddington accreting galactic microquasar SS433 ($\dot{M}_{\rm BH} = 10^{-4}$ $\mathrm{M}_\odot\ \mathrm{yr}^{-1}$; Fabrika 2004).

[3] This factor might be further exceeded in ULXs that are able to strongly beam their emission, for example magnetic neutron stars such as the object underlying M82-X2 (Bachetti et al. 2014).

3.3 Jet kinematics

The two VLA radio lobes have the same peak intensity (0.35 ± 0.06 mJy beam^{-1} and 0.34 ± 0.06 mJy beam^{-1}; Mezcua et al. 2013c) and distance to the compact source or X-ray position (arm-length ratio $R = 1.2$). This argues against nebular radio emission and indicates that the VLA radio lobes most likely belong to a radio jet that is either not significantly affected by Doppler boosting effects or whose velocity vector of the emitting plasma is very close to the plane of the sky. From the arm-length ratio and the angle-to-line of sight (θ), an estimate of the velocity in units of the speed of light (β) of a blob of plasma moving along the jet can be obtained from $\beta\cos\theta = (R-1)/(R+1)$ (Cseh et al. 2014). Based on the lobe flux ratio and arm-length ratio, we assume $\theta = 80^\circ$ and find $\beta = 0.4$, while the constraint of $\cos\theta \leq 1$ yields $\beta \geq 0.1$. Therefore, the velocity of the radio jet is constrained to 2.3×10^4–$1.2 \times 10^5\ \mathrm{km\,s}^{-1}$.

The localization of the IMBH in the spiral arm of a nearby galaxy suggests that it might have formed *in situ*, as IMBHs of 10^2–10^4 $\mathrm{M}_\odot$ are expected to form in dense young stellar clusters (Devecchi & Volonteri 2009). However, the $M_{\rm BH} = 5 \times 10^4$ $\mathrm{M}_\odot$ of NGC2276-3c appears too large for that. The main alternative is that NGC2276-3c is the nucleus of an accreted stripped dwarf galaxy, as is likely the case for ESO 243-49 HLX-1 (Farrell et al. 2012; Soria, Hau & Pakull 2013) and for the SMBH in the ultracompact dwarf galaxy M60-UCD1 (Seth et al. 2014). This is supported by the unusual morphology of the host spiral arm, its very high star formation rate (5–15 $\mathrm{M}_\odot\ \mathrm{yr}^{-1}$, Wolter et al. 2015) and the location of NGC 2276 in a galaxy group (Davis et al. 1997). Interestingly, in this scenario the presence of the two nearby luminous ULXs is readily explained as a result of the star formation triggered by the passage of the stripped dwarf galaxy nucleus through the spiral arm. The symmetrical VLA radio jet lobe structure implies that NGC2276-3c must be travelling at a slower rate than it takes to inflate the lobes so that when passing through NGC 2276 the lobes retain their shape and are not distorted by the galaxy's interstellar medium (ISM). Typical time-scales for minor merger passages are ∼1 Gyr (e.g. Lotz et al. 2010), with relative velocities between the two merging galaxies of 100–500 $\mathrm{km\,s}^{-1}$ (e.g. ∼200 $\mathrm{km\,s}^{-1}$ for HLX-1; Mapelli, Zampieri & Mayer 2012). From the jet expansion velocity and considering a distance between the compact core and the outer VLA radio lobes of ∼322 pc, a range of dynamic jet ages of ∼2500–14 000 yr is obtained. This means that the time-scale for forming the lobes ($t_{\rm lobe}$) is much lower than the time-scale of a dwarf galaxy passing through NGC 2276 ($t_{\rm pass}$). The jet radio morphology is expected to be distorted or to present a non-linear shape during the course of a merger event (e.g. as it is suggested in X-shaped radio galaxies; Merritt & Ekers 2002; Mezcua et al. 2011, 2012) unless $t_{\rm lobe} \ll t_{\rm pass}$. Hence, the finding that $t_{\rm lobe} \ll t_{\rm pass}$ and that the jet velocity is much larger than the IMBH/dwarf galaxy's velocity favours the scenario in which the IMBH is the nucleus of a stripped dwarf galaxy, and might explain the unusual morphology and high star formation in the spiral arm of NGC 2276.

3.4 Jet power, efficiency and feedback

An estimate of the total jet power, $Q_{\rm jet}$, can be derived from the radio luminosity of the compact jet. Using the correlation between core radio luminosity and kinetic power from Merloni & Heinz (2007), which has the minimum scatter (0.4 dex) and is based on a sample of sub-Eddington accreting SMBHs with flat-spectrum compact jet cores, we obtain $Q_{\rm jet} = 4 \times 10^{40}$ erg s^{-1}, which is of the same order as the bolometric luminosity of NGC2276-3c ($\sim 10^{40}$–10^{41} erg s^{-1}).

From the jet power and accretion rate, we can estimate the jet efficiency, or fraction of the accretion power that is used in the kinetic motion of the jet, $\eta_{\rm j} = Q_{\rm jet}/(\eta \dot{M}_{\rm BH} c^2)$, where $\eta = 10$ per cent. Jet efficiencies of $\sim$10 per cent or higher (e.g. Nemmen & Tchekhovskoy 2014) are estimated for massive radio galaxies, where the mechanical feedback from their jets produces cavities in their immediate intergalactic environment (e.g. McNamara & Nulsen 2007). This mode of mechanical jet feedback (the so-called radio mode) in SMBHs is thought to be equivalent to the low/hard state of XRBs with low Eddington accretion ratios (<2 per cent; e.g. Churazov et al. 2005). Using $Q_{\rm jet} = 4 \times 10^{40}$ erg s^{-1} and $\dot{M}_{\rm BH} = 1.5 \times 10^{-5}$ M$_\odot$ yr^{-1}, we obtain $\eta_{\rm j} = 46$ per cent. The jet efficiency would be even higher if we e.g. take $k_{\rm bol} = 1$ (this would yield $\dot{M}_{\rm BH} = 3 \times 10^{-6}$ M$_\odot$ yr^{-1} and $\eta_{\rm j} = 230$ per cent) or use the relationship from Cavagnolo et al. (2010). In all cases, the estimated jet efficiency of NGC2276-3c is as large as that from massive radio galaxies with radio-mode mechanical feedback, demonstrating that the physical mechanisms of jet production and energy dissipation are similar not only for stellar-mass and SMBHs (Nemmen et al. 2012) but also for IMBHs. In SMBHs, such feedback is predicted to prevent star formation in the inner core of their host galaxy (radius <0.1 kpc; Kim et al. 2011) and to increase the proportion of stars deposited farther away from the centre (e.g. Dubois et al. 2013). This scenario is consistent with the optical image of NGC2276-3c (Fig. 1b): a region of length $\sim$300 pc that is devoid of young stars is present in between the two peaks of the large-scale VLA radio lobes and oriented in the same direction as the parsec-scale EVN jet, while a larger population of stars is observed at the edges of the radio lobe emission. Randomly placing the VLA radio contours over other optical cavities observed in the *Hubble Space Telescope (HST)* image produces an obvious alignment in only 2 out of 19 trials, which makes a chance alignment between the optical cavity and the radio lobes unlikely (see also Mezcua et al. 2013c). Therefore, it is quite possible that the radio jet from the IMBH is clearing a cavity around it, in which new star formation is suppressed, while the star formation at the edges of this cavity could either take place when the material swept out by the jet collides with the ISM of NGC 2276 or have been triggered during the merger (e.g. Alonso-Herrero et al. 2012).

4 CONCLUSIONS

Finding a large number of IMBHs is pivotal for understanding the role they play in SMBH/galaxy formation. The discovery of an IMBH in the spiral arm of NGC 2276 indicates that, in addition to the low-mass galaxies, the brightest ULXs in nearby spirals and the nuclei of minor mergers remain amongst the best IMBH candidates. The finding that the jet kinetic power of NGC2276-3c is comparable to its radiative output and that its jet efficiency is as large as those of radio galaxies indicates that if seed BHs in the early Universe had powerful jets similar to that of NGC2276-3c; their jet mechanical feedback must be taken into account in cosmological simulations and studies of SMBH/galaxy growth.

ACKNOWLEDGEMENTS

MM acknowledges support from the Spanish Grant PNAYA2011-25527. TPR and ADS were funded as part of the STFC consolidated grants ST/K000861/1 and ST/L00075X/1. The authors thank Eduardo Ros and Rodrigo Nemmen for insightful discussion. We thank the *Chandra* X-ray Center for granting us a Director's Discretionary Time observation of NGC 2276. The EVN is a joint facility of European, Chinese, South African and other radio astronomy institutes funded by their national research councils.

REFERENCES

Alexander T., Natarajan P., 2014, Science, 345, 1330
Alonso-Herrero A., Rosales-Ortega F. F., Sánchez S. F., Kennicutt R. C., Pereira-Santaella M., Díaz Á. I., 2012, MNRAS, 425, L46
Bachetti M. et al., 2014, Nature, 514, 202
Cavagnolo K. W., McNamara B. R., Nulsen P. E. J., Carilli C. L., Jones C., Bîrzan L., 2010, ApJ, 720, 1066
Churazov E., Sazonov S., Sunyaev R., Forman W., Jones C., Böhringer H., 2005, MNRAS, 363, L91
Cseh D. et al., 2012, ApJ, 749, 17
Cseh D. et al., 2014, MNRAS, 439, L1
Cseh D. et al., 2015, MNRAS, 446, 3268
Davis D. S., Keel W. C., Mulchaey J. S., Henning P. A., 1997, AJ, 114, 613
Devecchi B., Volonteri M., 2009, ApJ, 694, 302
Dickey J. M., Lockman F. J., 1990, ARA&A, 28, 215
Dong X. et al., 2007, ApJ, 657, 700
Dubois Y., Devriendt J., Slyz A., Teyssier R., 2012, MNRAS, 420, 2662
Dubois Y., Gavazzi R., Peirani S., Silk J., 2013, MNRAS, 433, 3297
Fabrika S., 2004, Astrophys. Space Phys. Rev., 12, 1
Farrell S. A., Webb N. A., Barret D., Godet O., Rodrigues J. M., 2009, Nature, 460, 73
Farrell S. A. et al., 2012, ApJ, 747, L13
Gallo E., Miller B. P., Fender R., 2012, MNRAS, 423, 590
Gallo E. et al., 2014, MNRAS, 445, 290
Gladstone J. C., Roberts T. P., Done C., 2009, MNRAS, 397, 1836
Graham A. W., Scott N., 2013, ApJ, 764, 151
Greene J. E., Ho L. C., 2007, ApJ, 670, 92
Gültekin K., Cackett E. M., Miller J. M., Di Matteo T., Markoff S., Richstone D. O., 2009, ApJ, 706, 404
Gültekin K., Cackett E. M., King A. L., Miller J. M., Pinkney J., 2014, ApJ, 788, L22
Kim J.-h., Wise J. H., Alvarez M. A., Abel T., 2011, ApJ, 738, 54
Liu J.-F., Bregman J. N., Bai Y., Justham S., Crowther P., 2013, Nature, 503, 500
Lobanov A. P., 2005, preprint (arXiv:astro-ph/0503225)
Lotz J. M., Jonsson P., Cox T. J., Primack J. R., 2010, MNRAS, 404, 575
McNamara B. R., Nulsen P. E. J., 2007, ARA&A, 45, 117
Mapelli M., Zampieri L., Mayer L., 2012, MNRAS, 423, 1309
Marchese E., Della Ceca R., Caccianiga A., Severgnini P., Corral A., Fanali R., 2012, A&A, 539, A48
Merloni A., Heinz S., 2007, MNRAS, 381, 589
Merloni A., Heinz S., di Matteo T., 2003, MNRAS, 345, 1057
Merritt D., Ekers R. D., 2002, Science, 297, 1310
Mezcua M., Lobanov A. P., 2011, Astron. Nachr., 332, 379
Mezcua M., Prieto M. A., 2014, ApJ, 787, 62
Mezcua M., Lobanov A. P., Chavushyan V. H., León-Tavares J., 2011, A&A, 527, A38
Mezcua M., Chavushyan V. H., Lobanov A. P., León-Tavares J., 2012, A&A, 544, A36
Mezcua M., Farrell S. A., Gladstone J. C., Lobanov A. P., 2013a, MNRAS, 436, 1546
Mezcua M., Lobanov A. P., Martí-Vidal I., 2013b, MNRAS, 436, 2454
Mezcua M., Roberts T. P., Sutton A. D., Lobanov A. P., 2013c, MNRAS, 436, 3128

Mezcua M., Fabbiano G., Gladstone J. C., Farrell S. A., Soria R., 2014, ApJ, 785, 121
Middleton M. J. et al., 2013, Nature, 493, 187
Migliari S., Fender R., 2005, Ap&SS, 300, 197
Miller-Jones J. C. A. et al., 2012, ApJ, 755, L1
Mineshige S., Ohsuga K., 2011, Astron. Nachr., 332, 402
Mortlock D. J. et al., 2011, Nature, 474, 616
Motch C., Pakull M. W., Soria R., Grisé F., Pietrzyński G., 2014, Nature, 514, 198
Nemmen R. S., Tchekhovskoy A., 2014, preprint (arXiv:1406.7420)
Nemmen R. S., Georganopoulos M., Guiriec S., Meyer E. T., Gehrels N., Sambruna R. M., 2012, Science, 338, 1445
Pakull M. W., Soria R., Motch C., 2010, Nature, 466, 209
Pasham D. R., Strohmayer T. E., Mushotzky R. F., 2014, Nature, 513, 74
Plotkin R. M., Markoff S., Kelly B. C., Körding E., Anderson S. F., 2012, MNRAS, 419, 267
Reines A. E., Greene J. E., Geha M., 2013, ApJ, 775, 116
Rushton A., Spencer R., Fender R., Pooley G., 2010, A&A, 524, A29
Schramm M. et al., 2013, ApJ, 773, 150
Seth A. C. et al., 2014, Nature, 513, 398
Soria R., Hau G. K. T., Pakull M. W., 2013, ApJ, 768, L22
Soria R., Long K. S., Blair W. P., Godfrey L., Kuntz K. D., Lenc E., Stockdale C., Winkler P. F., 2014, Science, 343, 1330
Sutton A. D., Roberts T. P., Walton D. J., Gladstone J. C., Scott A. E., 2012, MNRAS, 423, 1154
Sutton A. D., Roberts T. P., Middleton M. J., 2013, MNRAS, 435, 1758
Terashima Y., Wilson A. S., 2003, ApJ, 583, 145
Thornton C. E., Barth A. J., Ho L. C., Rutledge R. E., Greene J. E., 2008, ApJ, 686, 892
Vasudevan R. V., Fabian A. C., 2009, MNRAS, 392, 1124
Volonteri M., 2010, A&AR, 18, 279
Volonteri M., Silk J., 2014, preprint (arXiv:1401.3513)
Webb N. et al., 2012, Science, 337, 554
Wolter A., Esposito P., Mapelli M., Pizzolato F., Ripamonti E., 2015, preprint (arXiv:1501.01994)
Wolter A., Pizzolato F., Rota S., Mapelli M., Ripamonti E., 2011, Astron. Nachr., 332, 358
Wrobel J. M., Ho L. C., 2006, ApJ, 646, L95
Wrobel J. M., Greene J. E., Ho L. C., Ulvestad J. S., 2008, ApJ, 686, 838
Yuan W., Zhou H., Dou L., Dong X.-B., Fan X., Wang T.-G., 2014, ApJ, 782, 55

This paper has been typeset from a TEX/LATEX file prepared by the author.